Separation Science and Technology
Publication details, including instructions for authors and subscription information:
http://www.informaworld.com/smpp/title~content=t713708471

Equilibrium Analysis of Cyclic Adsorption Processes: CO_2 Working Capacities with NaY

P. J. E. Harlick[a]; F. H. Tezel[a]
[a] Department of Chemical Engineering, University of Ottawa, Ottawa, Ontario, Canada

To cite this Article Harlick, P. J. E. and Tezel, F. H.(2005) 'Equilibrium Analysis of Cyclic Adsorption Processes: CO_2 Working Capacities with NaY', Separation Science and Technology, 40: 13, 2569 — 2591
To link to this Article: DOI: 10.1080/01496390500283233
URL: http://dx.doi.org/10.1080/01496390500283233

Separation Science and Technology, 40: 2569–2591, 2005

ISSN 0149-6395 print/1520-5754 online
DOI: 10.1080/01496390500283233

Equilibrium Analysis of Cyclic Adsorption Processes: CO_2 Working Capacities with NaY

P. J. E. Harlick and F. H. Tezel
Department of Chemical Engineering, University of Ottawa,
Ottawa, Ontario, Canada

Abstract: The most common application of adsorption is via pressure swing adsorption. In this type of design, the feed and regeneration temperatures are kept approximately equal, whereas the feed pressure is higher than the regeneration pressure. By exploiting the difference in the amount adsorbed at a higher pressure to the amount adsorbed at a lower pressure, a working capacity is realized. Therefore, by examining the expected (ideal) working capacity of an adsorbent, a performance characteristic can be analyzed for a pressure swing adsorption process (PSA). For this work, feed pressures up to 2.0 atm CO_2 and feed temperatures from 20°C to 200°C were investigated. These limits were chosen due to the nature of the target process: CO_2 removal from flue gas.

Carbon dioxide adsorption isotherms were determined in a constant volume system at 23°C, 45°C, 65°C, 104°C, 146°C, and 198°C, for pressures between 0.001 and 2.5 atm CO_2 with NaY zeolite. These data were fit with the temperature dependent form of the Toth isotherm. Henry's Law constants and the heat of adsorption at the limit of zero coverage were also determined using the concentration pulse method. Comparison of the Henry's Law constants derived from the Toth isotherm, and those obtained with the concentration pulse method provided excellent agreement.

By using the Toth isotherm, expected working capacity contour plots were constructed for PSA (Pressure Swing Adsorption), TSA (Temperature Swing Adsorption), and PTSA (Pressure Temperature Swing Adsorption) cycles. The largest expected working capacities were obtained when the bed was operated under a high-pressure gradient PSA cycle, or a high thermal and pressure gradient PTSA cycle. The results

Received 28 October 2003, Accepted 5 July 2005

Address correspondence to F. H. Tezel, Department of Chemical Engineering, University of Ottawa, 161 Louis-Pasteur, Ottawa, Ontario, Canada K1N 6N5. Tel.: 1 (613) 562-5800 Ext. 6099; Fax: 1 (613) 562-5172; E-mail: tezel@eng.uottawa.ca

also showed that certain TSA and PSA cycle conditions would result with higher expected working capacities as the feed temperature increases.

Keywords: Carbon dioxide separation from flue gas, carbon dioxide adsorption, NaY zeolite, pressure swing adsorption, temperature swing adsorption, pressure temperature swing adsorption

INTRODUCTION

Although CO_2 is emitted by several sources (including *natural*, *residential*, *automotive*, *industrial*), the industrial sector has been targeted by global concerns and politicians. In order to meet the present and future constraints placed on the allowable emissions of CO_2 the solution lies with point source reduction and recovery. Therefore, a treatment process must be developed. For this treatment process to succeed, it must be capable of effective and efficient removal, concentration, and recovery of CO_2 from flue gas for industrial applications.

Presently, there are several technologies available for removing these gases from the exhaust streams before release to the atmosphere (1). Absorption, cryogenic distillation, fixation by biotechnology, membrane-based processes, and adsorption are possible separation methods. Only adsorption-based processes are examined in this study.

Adsorption-based systems are commonly designed around isobaric or isothermal modes of operation. The separation is based on a kinetic or equilibrium difference of the components on a specific or blend of adsorbents. Although the process is viable for large-scale separations, if the process is not properly designed, the setup will not be able to deal with widely changing inlet conditions.

Adsorption is a process that involves the fixation of a mixture or component (*adsorbate*(*s*)) to the surface of a solid (adsorbent). A separation can be achieved by exploiting either kinetic or equilibrium properties of the components within the adsorbent.

In order to exploit the adsorption properties of adsorbents, the adsorbent must be utilized within a process. This process should exploit the difference in adsorption capacities or component kinetics exhibited by differences in operating conditions. In the field of adsorption, there are three main process concepts:

1. Pressure Swing Adsorption (PSA)
2. Temperature Swing Adsorption (TSA)
3. Pressure Temperature Swing Adsorption (PTSA)

All other variations of adsorption unit operations are based on one of the previous three process concepts. An extensive review and teaching of the adsorption-based process is given by Cen and Yang (2), Yang (3), Kumar and Van Sloun (4), White and Barkley (5), Ruthven et al. (6).

In the art of adsorption separations, the pressure swing process is most widely employed (7–17). Recent advances in the design of PSA systems

have also greatly enhanced the productivity and capabilities of the separation scheme (15, 16, 18).

The process is based on exploiting the difference in adsorption capacity exhibited by an adsorbate-adsorbent system when step changes in the operating pressure are applied; the difference in adsorption capacity is termed the working capacity. The expected working capacity is difference in the amount adsorbed at the feed pressure and the regeneration pressure obtained from an adsorption isotherm. With this approach, the product purity is highly dependent on the conditions used to obtain the low pressure (17). In many PSA processes, the desired product is the less adsorbed component, where the more adsorbed component is discarded with no concern of purity. An example of this type of system is natural gas upgrading. The N_2 and CH_4 are generally weakly adsorbed, whereas the CO_2 and other heavy components are strongly adsorbed (11). These more adsorbed components are then desorbed and released to incineration or to the atmosphere during the regeneration stage of the process.

Several factors affect the operation of the PSA process. These include particle size and composition effects (19, 20), bed pressure drop (21), heat effects (22), feed conditions (23), incomplete regeneration (24), feed pressure, temperature, and adsorbent characteristics. All of these factors must be considered prior to the design of a PSA process.

In our previous work (25) a series of various adsorbents were studied and screened according to the N_2 and CO_2 heat of adsorption, Henry's Law constants, and for selected adsorbents the isotherms at 23°C. From the set of 13 adsorbents, the NaY adsorbent was chosen for further study and is the focus of this work.

ISOTHERM MODEL

In order to reduce experimental data to a set of parameters, the three-parameter Toth isotherm may be used and is given by Eq. (1)

$$q = \frac{q_m b P}{(1 + bP^t)^{1/t}} \tag{1}$$

The parameters q_m, b, and t may also be expressed as a function of temperature and are given by Eqs. (2)–(4), respectively (26).

$$q_m = q_{m_0} exp\left(\chi\left(1 - \frac{T_0}{T}\right)\right) \tag{2}$$

$$b = b_0 exp\left(\frac{Q}{RT_0}\left(\frac{T_0}{T} - 1\right)\right) \tag{3}$$

$$t = t_0 + \alpha\left(1 - \frac{T_0}{T}\right) \tag{4}$$

The parameter Q represents the isosteric heat of adsorption when evaluated at the limit of zero fractional loading.

The Toth isotherm also allows for determining the Henry's Law constant, Eq. (5), and the heat of adsorption as a function of loading, Eq. (6)

$$K_p = q_m b \tag{5}$$

$$(-\Delta H) = Q - \frac{1}{t}(\alpha R T_0)\left\{ln\left(\frac{\theta}{(1-\theta^t)^{1/t}}\right) - \frac{ln(\theta)}{(1-\theta^t)}\right\} \tag{6}$$

where q_m, b, and t are given by Eqs. (2)–(4), respectively.

By using these relationships, Eqs. (1)–(4), a combined nonlinear regression of the experimental data can be performed, and a three-dimensional (q, P, T) relationship can be determined. By using this relationship, several ideal PSA cycles can be studied, where the expected working capacity is identified as an indicator of performance. The expected working capacity (EWC) is easily defined by the following general equation.

$$EWC = q(P_F, T_F) - q(P_R, T_R) \tag{7}$$

Therefore, by setting any combination of two of the design parameters, the feed pressure or temperature, or the regeneration pressure or temperature, working capacity contours can be generated. By constructing these plots under various conditions, the effects of the isotherm shape and operating conditions on the expected working capacity of the adsorbent can be determined and used as part of the screening criteria. For example, under equal feed and regeneration temperatures, PSA equilibrium cycles could be studied. When equal feed and regeneration pressures are implied, then TSA equilibrium cycles could be studied. Similarly, by varying the temperature and pressure of the feed or regeneration cycle, then PTSA equilibrium cycles could be studied.

EXPERIMENTAL METHOD

The experimental approach used in this study consisted of a constant volume system for determining the various isotherms and a modified gas chromatograph for determining the Henry's Law constants (K_p) via the Concentration Pulse Method (CPM). Schematic diagrams of each of the experimental apparatus are shown in Figs. 1 and 2. The experimental and column characteristics used with the CPM are given in Table 1.

The volumetric method is based on the principle of constant volume and temperature where changes in pressure are measured. These pressure changes are proportional to the amount adsorbed and are easily calculated using the ideal gas law. A modified Micromeretics Accusorb 2400 volumetric unit was used for determining the pure component isotherms.

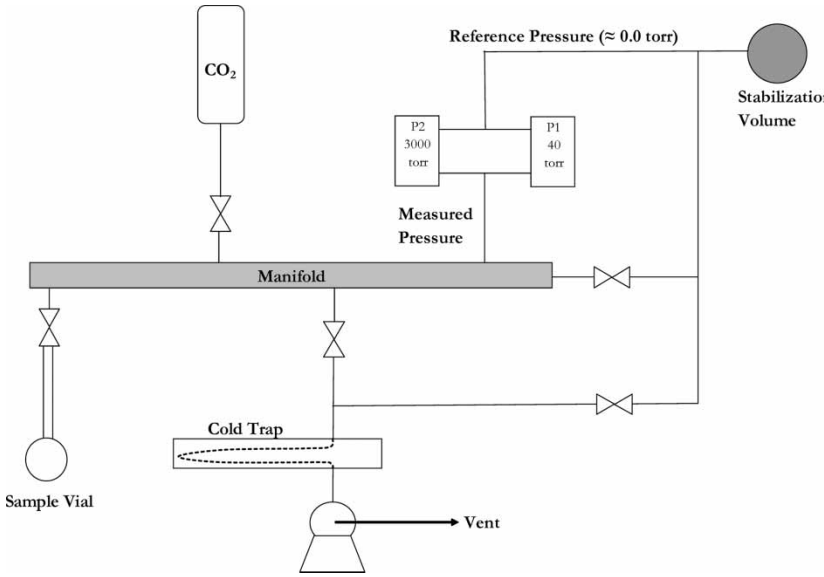

Figure 1. Constant volume setup used for determining the adsorption isotherms.

The concentration pulse method (CPM) was used for determining the Henry's Law constants (27–38). As shown in Fig. 2, the flowrate (**A**) was controlled by a MKS mass flow controller (*MFC*), model number 1359 (0–50 sccm range), and set to a total helium flowrate of 40 cc/min at the given temperature.

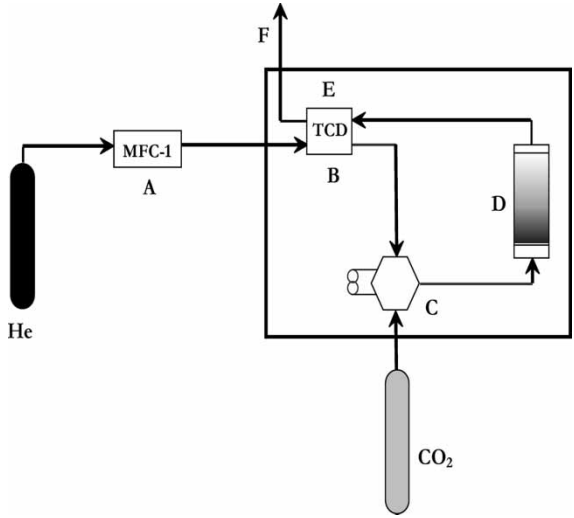

Figure 2. CPM setup used for determining the Henry's Law constants.

Table 1. Column characteristics used with the CPM

Carrier gas	UHP Helium
Particle size	20 × 60 mesh
Average particle diameter	545 μm
Bed porosity	0.382
Column length	24.75 cm
Total flow-rate	40.0 cc/min@40°C
Total pressure	1.0 atm.
Regeneration temperature	200 °C
Regeneration pressure	1.0 atm.
Regeneration time	12 hours

The carrier gas was then passed through the reference side of the TCD contained in the GC (**B**). This TCD was used to measure the response of the column to the sample injection (**C**). After the injection, the carrier and sample passed through the packed column (**D**) and the response was measured (**E**) and vented to the atmosphere (**F**).

Data acquisition was performed using *National Instruments*-based data acquisition card and *Labview v6.1* on an Intel-based computer. A column was packed with the NaY adsorbent (*20–60 mesh, provided by UOP*) and was contained within a modified *Varian 3400* gas chromatograph. The *GC* was equipped with a high-sensitivity thermal conductivity detector.

From the results of our previous work (25), the NaY adsorbent was selected for further study. This adsorbent was provided by UOP as 1/16″ extrudate. For the purposes of determining the CO_2 isotherms at various temperatures, the adsorbent was used as supplied.

Before the start of each CPM experimental run, the adsorbent was regenerated at 1.0 atmosphere total pressure and 200°C under a 40 sccm helium purge, for approximately 12 h. For the constant volume method, the adsorbent was regenerated at 10^{-4} torr and 200°C for approximately 12 h.

NUMERICAL METHODS

In order to determine the parameters for the pure component fits to the temperature-dependent form of the Toth isotherm, a nonlinear regression was performed, considering all the data points at different temperatures. This approach was based on a Generalized Reduced Gradient (GRG2) nonlinear optimization code. Quadratic extrapolation was employed to obtain initial estimates of the basic variables in each one-dimensional search. The Jacobian for the objective and constraint functions was approximated by a central finite difference approach. A quasi-Newton iteration method was also used. Tolerance and convergence were each set at 1.0E-9. The solution was taken when no further change in the sum of square residuals could be

obtained for a wide range of starting values. This wide range of initial guesses ensured that the absolute, not the local minimum, was obtained. This nonlinear regression was programmed on an Excel spreadsheet.

RESULTS

In order to determine the effect that the isotherm shape has on the expected performance of the adsorbent in an adsorption cycle, various temperatures were used and the corresponding CO_2 adsorption isotherms were determined. The temperatures were chosen so that various points of interest were used. These included the base (reference) temperature of 23°C, and 45°C, 65°C, 104°C, 146°C, and 198°C. The results of the CO_2 adsorption isotherms are given in Fig. 3, shown on a log-log scale for low-pressure clarity. The Toth isotherm regression parameters and results are shown in Table 2. As can be seen from this table, q_m was not a function of temperature, since χ was determined to be 0 as a result of the nonlinear regression.

As expected, the adsorption capacity decreased with increasing temperature; however, it is important to note that the isotherm shape also changes drastically. At low temperatures, the isotherm assumes a rectangular shape,

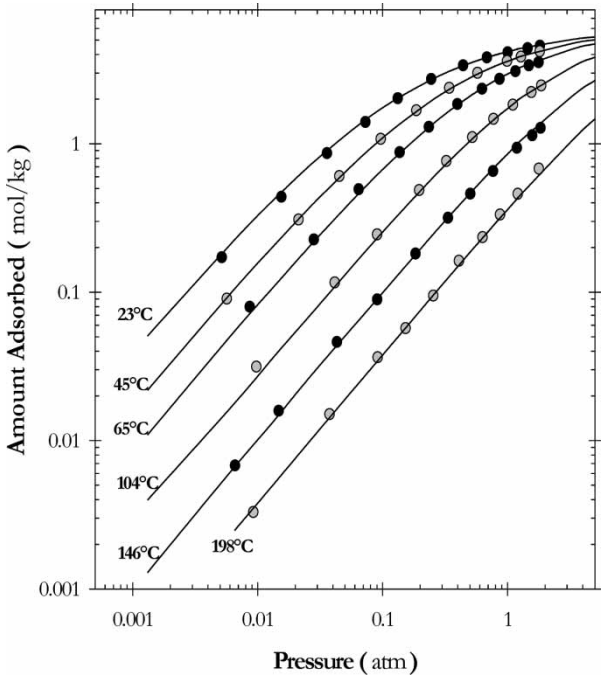

Figure 3. NaY adsorption isotherms with CO_2. Curves represent the temperature dependent Toth isotherm fits.

Table 2. Toth isotherm parameters for CO_2 with NaY

Temperature (K)	Isotherm fit			Quality of fit (SSR)	Temperature dependent parameters
	q_m (mmol/g)	b (1/atm)	t (dimensionless)		
296	8.3	9.9	0.48	1.0E-02	$b_0 = 9.9$
318	8.3	3.5	0.54	1.8E-03	$Q/RT_0 = 15$
338	8.3	1.6	0.60	9.2E-03	$q_{m0} = 8.3$
377	8.3	0.41	0.69	7.2E-03	$\chi = 0$
419	8.3	0.13	0.77	9.2E-03	$t_0 = 0.48$
471	8.3	0.040	0.85	1.8E-03	$\alpha = 1.0$

whereas at higher temperatures the isotherms tend more to linearity. These features are expected to play an important role in defining the expected working capacity.

By using the temperature-dependent form of the Toth isotherm [Eqs. (1)–(4)], the results of the regression are shown as solid lines at various temperatures in Fig. 3. The results show an excellent fit with the experimental data. Therefore, it may be assumed that the Toth isotherm can be used as an accurate model of the CO_2 adsorption equilibrium.

Henry's Law constants for CO_2 in NaY were also studied at various temperatures by using the concentration pulse method (CPM) and compared to the ones obtained by Toth isotherms in Fig. 4 as a van't Hoff plot. The symbols represent the CPM data and the line represents the values found by Eq. (5) from the Toth isotherms. As can be seen from this figure, the agreement for these different methods is very good.

Since the Toth isotherm can be used to model the CO_2 adsorption on NaY, various cyclic adsorption processes were examined. It is important to note that the following are based on an equilibrium study of the adsorption process as applied to the cyclic nature of practical adsorption. Therefore, in the following PSA, TSA, and PTSA cycles, it is assumed that equilibrium has been attained in each of the feed and regeneration phases. It was also assumed that the adsorption and regeneration phases are carried out as isothermal processes for the PSA. The temperature usually increases during adsorption, due to the exothermic nature of adsorption, and decreases during desorption. When a rough estimate of the energy balance was completed for this system, it was seen that the temperature increased only by a few degrees in the column during adsorption. Therefore the assumption of isothermal PSA was justified.

Pressure Swing Adsorption (PSA)

The most common application of adsorption is via pressure swing adsorption. In this type of design, the feed and regeneration temperatures are kept

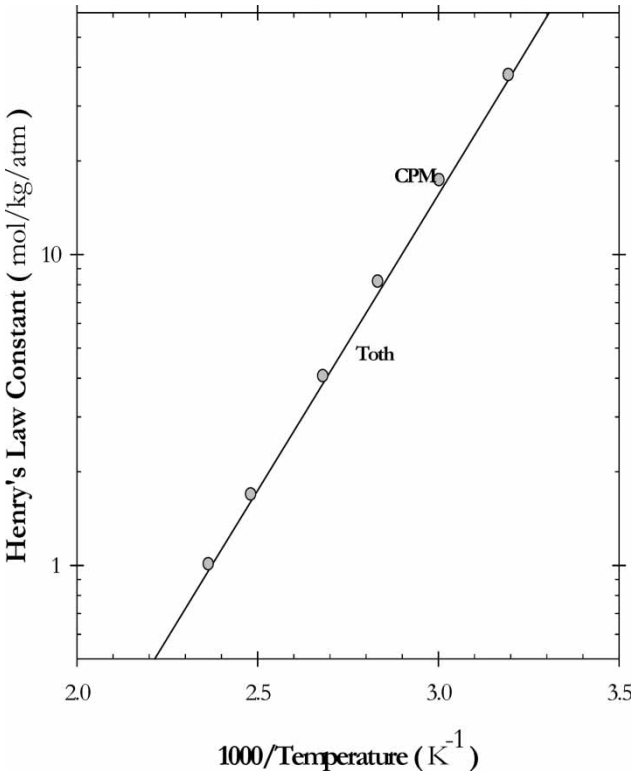

Figure 4. Comparison of the Henry's Law constants determined by the CPM, and the Toth isotherm.

approximately equal, whereas the feed pressure is higher than the regeneration pressure. By exploiting the difference in the amount adsorbed at the higher pressure and the amount adsorbed at the lower pressure at constant bed temperature, a working capacity is realized [Eq. (7)]. Therefore, by examining the expected (ideal) working capacity of an adsorbent, its performance characteristics can be analyzed. For this work, feed pressures of up to 2.0 atm CO_2, and feed temperatures from 20°C to 200°C were investigated. These limits were chosen due to the nature of the target process: CO_2 removal from flue gas.

The results of simulated equilibrium-based PSA cycles are shown in Figs. 5 through 7. For a feed and regeneration temperature of 25°C, the resulting expected CO_2 working capacities are shown as a filled contour plot in Fig. 5. The contours show that the working capacity increase follows a log-based decrease in the regeneration pressure, or increase in the feed pressure, which is expected.

Using these contours for PSA performance for the NaY adsorbent with CO_2, higher bed temperatures were examined. Comparison of 25°C and

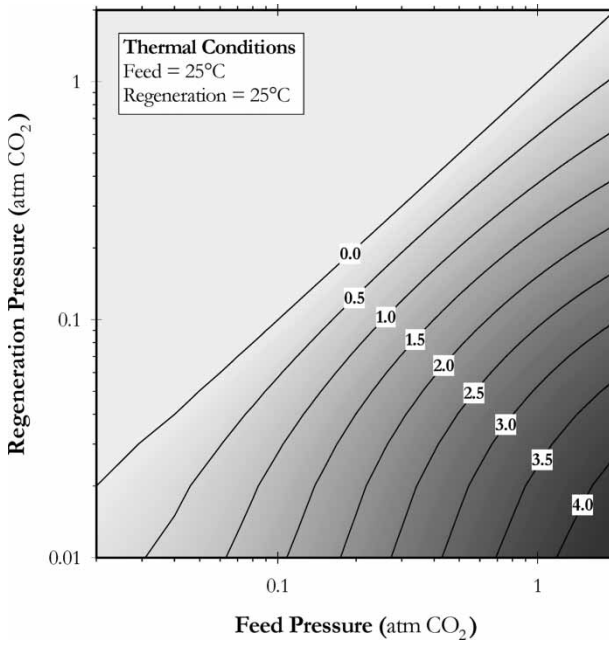

Figure 5. PSA expected working capacity (mol/kg) for a bed temperature of 25°C.

50°C bed temperatures are shown in Fig. 6. The results show that the PSA performance at 50°C exhibits higher expected working capacities than those found at 25°C, for certain conditions. For example, when the bed is operated in the range to the right of the line shown in Fig. 6 (shown as arrows), the expected working capacity is higher at 50°C than 25°C. This type of behaviour is purely based on the effect that the isotherm shape exhibits on the operating performance. However, as the bed temperature is increased further, up to 100°C, the available operating region of higher expected working capacity for higher temperature has decreased (as can be seen as the region to the right of the cross-over line, shown as arrows in Fig. 7). The crossover between the two bed temperatures (25°C and 100°C) in Fig. 7 happens at higher feed and regeneration pressures than that obtained between the 25°C and 50°C bed temperatures, shown in Fig. 6. The most important feature of these results is that the expected working capacity can be enhanced by traditional reasoning, low regeneration–high feed bed pressures, but further improvements can be realized by increasing the bed temperature at higher regeneration pressures for PSA. Since the expected working capacity is defined as the difference in adsorption capacities at the feed and regeneration conditions, rather than the absolute value of the capacity itself, it is possible to have higher expected working capacities at higher temperatures. The slope of the adsorption equilibrium isotherms

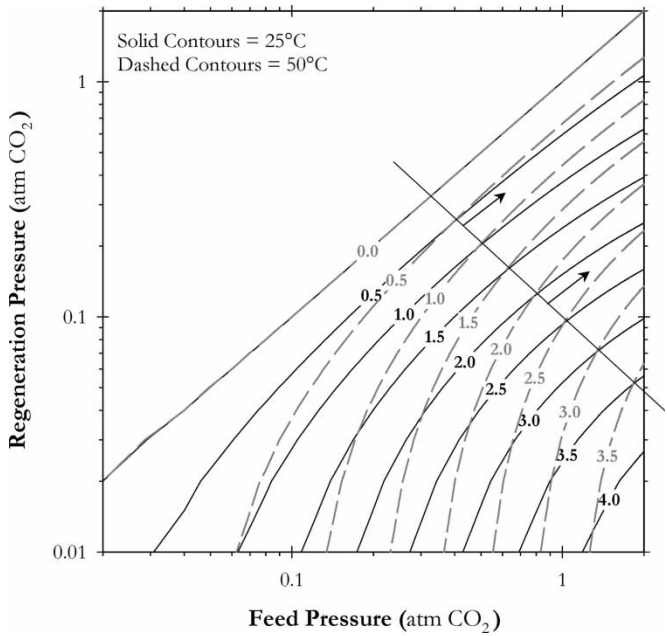

Figure 6. PSA expected working capacity (mol/kg) for bed temperatures of 25 and 50°C.

changes with pressure, as well as temperature. Therefore, although the absolute value of adsorption capacities decreases with increasing temperature, it is possible (under certain circumstances, depending on how the slope of the isotherm changes with respect to pressure and temperature) to have higher expected working capacities at higher bed temperatures.

This conclusion is very significant, especially for flue gas applications at high temperatures. It will not be necessary to cool them down too much, to carry out the adsorption separation of carbon dioxide. It is possible to have high expected working capacities at high temperatures, even without having to go down to very high vacuum for regeneration. This will have an impact on the economic viability of the PSA for this separation application. When the optimization of the operating conditions is carried out, the cost of cooling the flue gas has to be weighed against the increased cost of high-temperature material construction and power requirements.

Temperature Swing Adsorption (TSA)

Another application of adsorption is via temperature swing adsorption. In this type of design, the feed and regeneration pressures are kept approximately equal, whereas the feed temperature is lower than the regeneration

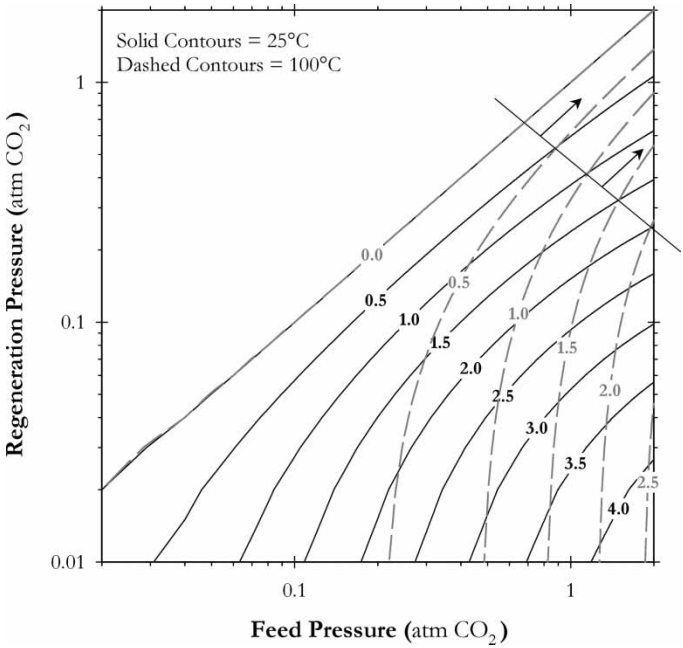

Figure 7. PSA expected working capacity (mol/kg) for bed temperatures of 25 and 100°C.

temperature. By exploiting the difference in the amount adsorbed at the lower temperature and the amount at the higher temperature, at constant bed pressure, a working capacity is realized. Therefore, by examining the expected (ideal) working capacity of an adsorbent, a performance characteristic can be analyzed. For this work, feed pressures up to 2.0 atm CO_2 and feed temperatures from 20°C to 200°C were investigated.

The results of the simulated equilibrium-based TSA cycles are shown in Figs. 8 through 10. For a feed and regeneration pressure of 0.15 atm CO_2 (15% CO_2 in air at 1.0 atm total pressure), the resulting expected CO_2 working capacity is shown as a filled contour plot in Fig. 8. The contours show that the working capacity increases as the feed temperature decreases. The nature of the contours also shows that for a given feed temperature, regeneration temperature does not affect the expected working capacities, especially at high feed temperatures, for this particular system. This indicates that any further increase in the regeneration temperature will not affect the cyclic expected working capacity. It will not be economically feasible to increase the regeneration temperature further.

Using these contours for TSA performance for the NaY adsorbent with CO_2, higher bed pressures were studied. Comparison of 0.15 and 1.0 atm CO_2 partial pressures are shown in Fig. 9. It shows that the increase in bed

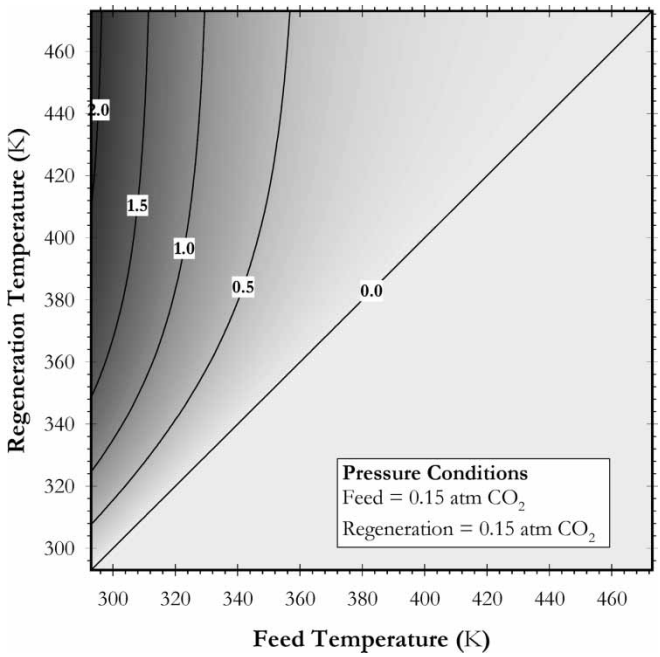

Figure 8. TSA expected working capacity (mol/kg) for partial pressure of 0.15 atm CO_2.

pressure will result with significantly higher expected working capacities for most feed temperatures studied. If the feed is at high pressure, it needs to be taken advantage of. However, at low feed and regeneration temperatures, the effect of the increased bed pressure is minimal. There is even a region at the lower-left corner in Fig. 9 (shown as arrow), where it is possible to get slightly higher expected working capacities at lower bed pressures. The explanation for this is the same as the possibility of getting higher expected working capacities with higher bed temperatures (see the previous PSA section). It depends on how the slope of the isotherm changes with pressure and temperature.

To further examine the effect of bed pressure on the TSA performance, 0.75 atm CO_2 partial pressure cycles were studied and compared to 1.0 atm CO_2 partial pressure cycles, and are shown in Fig. 10. The results shown in this figure indicate that an increase of 0.25 atm CO_2 pressure will have a slight effect on the TSA cyclic performance. At low regeneration and feed temperatures, the expected working capacities obtained at 0.75 atm and 1.0 atm CO_2 bed pressure resulted in no practical differences. At high regeneration and feed temperatures, the cyclic capacities are slightly higher for the higher bed pressure. But since the difference is not much, it will not be economically viable to increase the pressure within this range.

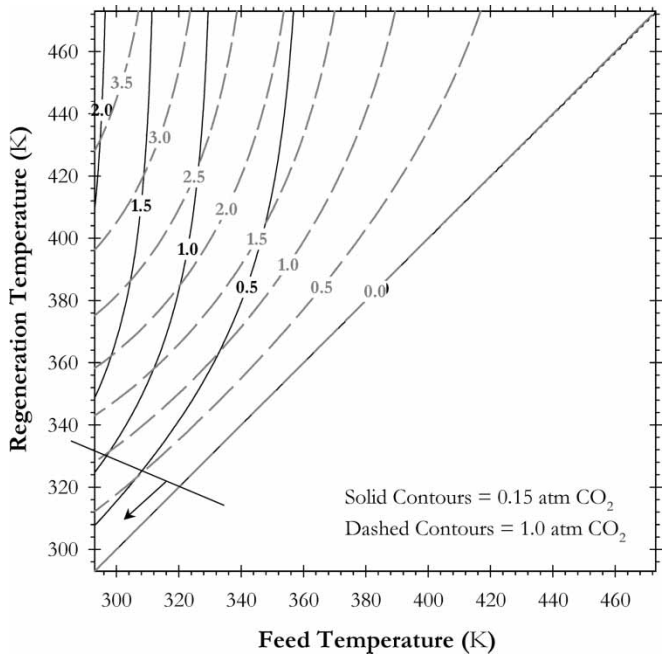

Figure 9. TSA expected working capacity (mol/kg) for partial pressure of 0.15 and 1.0 atm CO_2.

Pressure-Temperature Swing Adsorption (PTSA)

Another application of adsorption is via the combined pressure-temperature swing adsorption. In this type of design, both the pressure and the temperature in the bed are allowed to vary. Therefore, the bed experiences externally induced pressure and thermal shocks during a complete cycle. This presents a 4D problem that cannot be visualized simultaneously. Therefore, the results were organized according to feed variation and then regeneration variation. These results are shown in Figs. 11–17. The results for feed variations at constant regeneration conditions are given in Figs. 11–13. The results for regeneration variations are given in Figs. 14–17. For the discussions of this kind of a process, it is assumed that the process is not carried out at constant pressure (like TSA) or at constant temperature (like PSA). The feed and regeneration conditions are allowed to be different from each other. For the regeneration, the pressure, as well as the temperature, is allowed to be changed to get the maximum ideal expected working capacity.

For the case when the regeneration pressure was low, 0.001 atm CO_2, the effect of the PTSA cyclic exhibited no effect of regeneration temperature, as shown in Fig. 11. This is due to the shape factor of the isotherms, and the relative amount adsorbed at the regeneration pressure. As the regeneration

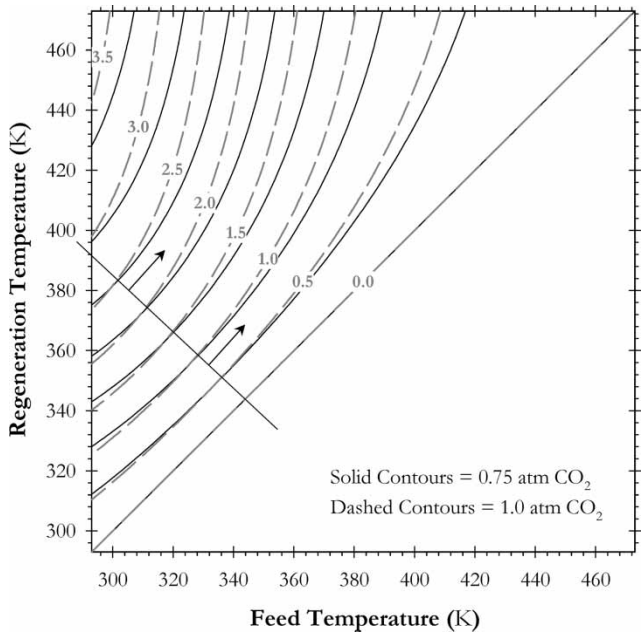

Figure 10. TSA expected working capacity (mol/kg) for partial pressure of 0.75 and 1.0 atm CO_2.

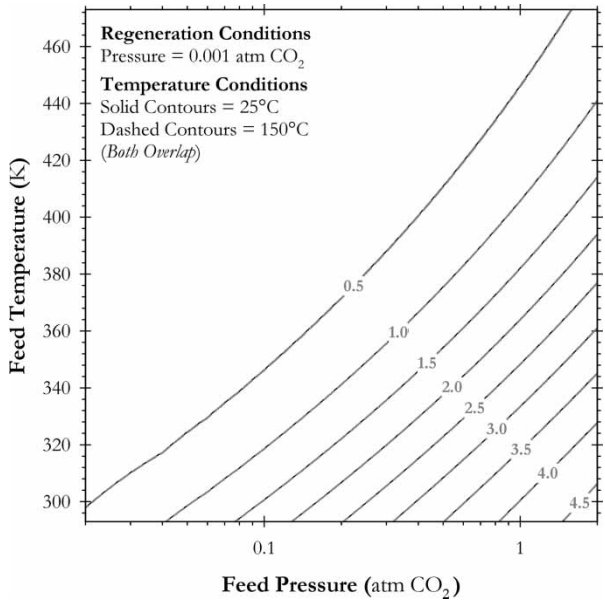

Figure 11. PTSA expected working capacity (mol/kg) for feed condition variation with a regeneration pressure of 0.001 atm CO_2.

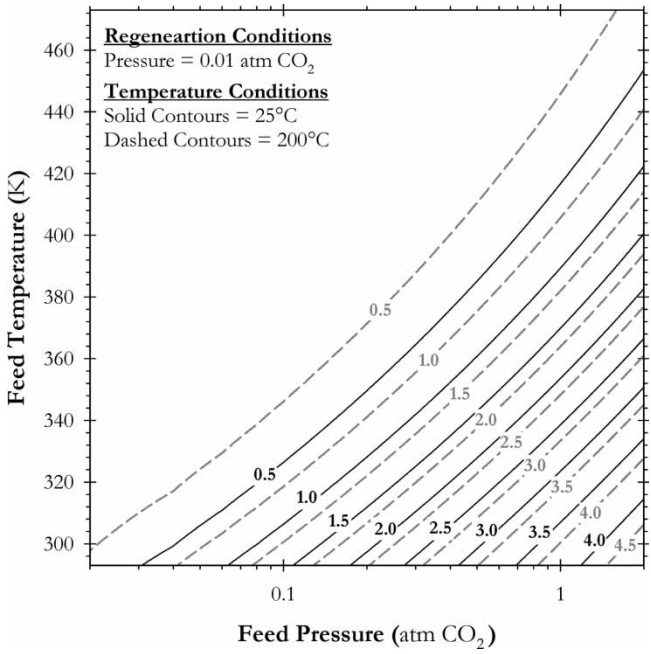

Figure 12. PTSA expected working capacity (mol/kg) for feed condition variation with a regeneration pressure of 0.01 atm CO_2.

pressure was increased to 0.01 atm CO_2, Fig. 12, the effects are seen as the regeneration temperature was increased to 200°C. The increase in regeneration temperature resulted with an increase in the expected working capacity, where for a given feed pressure the same expected working capacity could be realized with a higher feed temperature. However, the relative increase in the feed temperature condition does not translate into an equivalent amount of working capacity, given the large increase in the regeneration temperature.

As the regeneration pressure is further increased to 0.05 atm CO_2, the magnitude of the working capacity differences between increases in the regeneration temperature became larger, as shown in Fig. 13. When the bed is regenerated at 25°C, the expected working capacity decreases by over 0.5 mol/kg when compared to the expected working capacity at a regeneration temperature of 50°C. The further increase in regeneration temperature increases the expected working capacity under the same feed pressure and feed temperature conditions.

The simulated results for the PTSA cycles under regeneration variation are shown in Figs. 14–17. For a feed pressure of 0.15 atm CO_2, and feed temperatures of 25°C and 50°C, the cyclic capacities are shown and compared in Fig. 14. The results show that the process path to follow, in order to

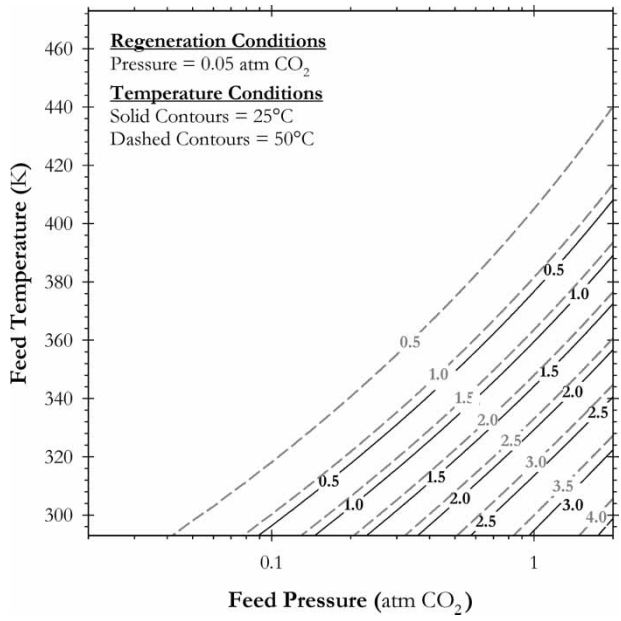

Figure 13. PTSA expected working capacity (mol/kg) for feed condition variation with a regeneration pressure of 0.05 atm CO_2.

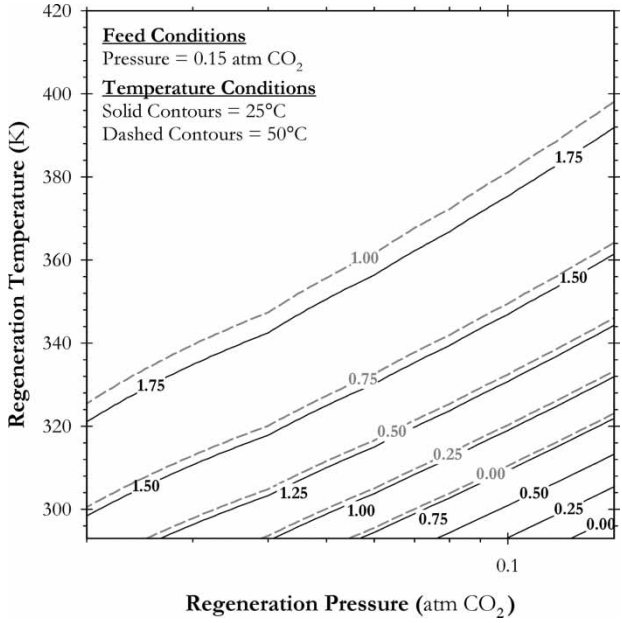

Figure 14. PTSA expected working capacity (mol/kg) for feed condition variation with a regeneration pressure of 0.15 atm CO_2.

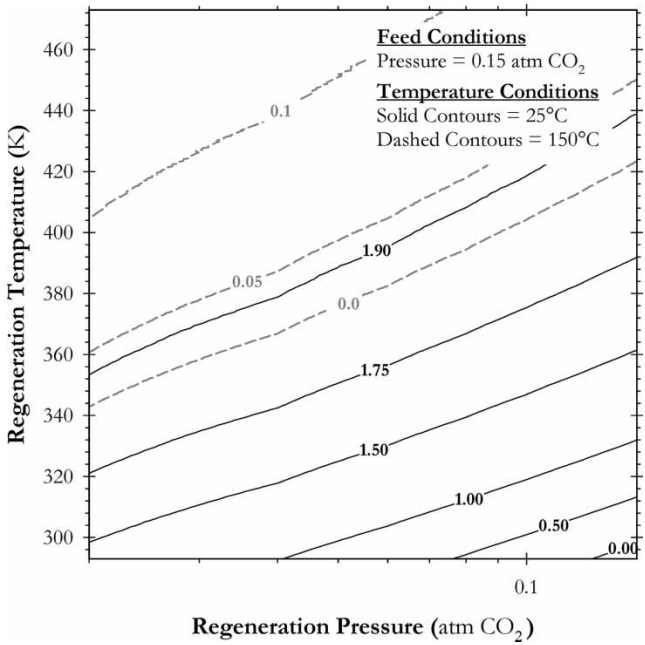

Figure 15. PTSA expected working capacity (mol/kg) for regeneration condition variation with a feed pressure of 0.15 atm CO_2.

increase the working capacity, is to keep the regeneration pressure high and increase the regeneration temperature. By following this path, the working capacity will increase at the steepest accent. The difference between operating the bed at 25°C and 50°C shows that the expected working capacity is higher at the lower bed temperature, as expected.

As the bed temperature was further increased to 150°C, the effects of operating at a low pressure became evident, as shown in Fig. 15. The expected working capacities at a bed temperature of 150°C are significantly lower than those obtained at 25°C. Therefore, operating the bed at low pressure and higher temperature will not produce a very efficient use of the adsorbent.

With further increases in the bed pressure, to 0.45 atm CO_2, the effects of the bed temperature are shown in Fig. 16 for 25°C and 50°C. The resulting shapes of the expected working capacity contours are almost identical, where a 1.0 mol/kg difference was found. Under these conditions, the effect of an increase in bed temperature require 40–80 K increase in the regeneration temperature or up to 80% decrease in the regeneration pressure in order to realize the equivalent expected working capacity.

As the feed pressure was further increased to 1.0 atm CO_2 (shown in Fig. 17), the difference in the expected working capacity contours increased as the feed temperature increased from 25°C to 50°C. In this case, the

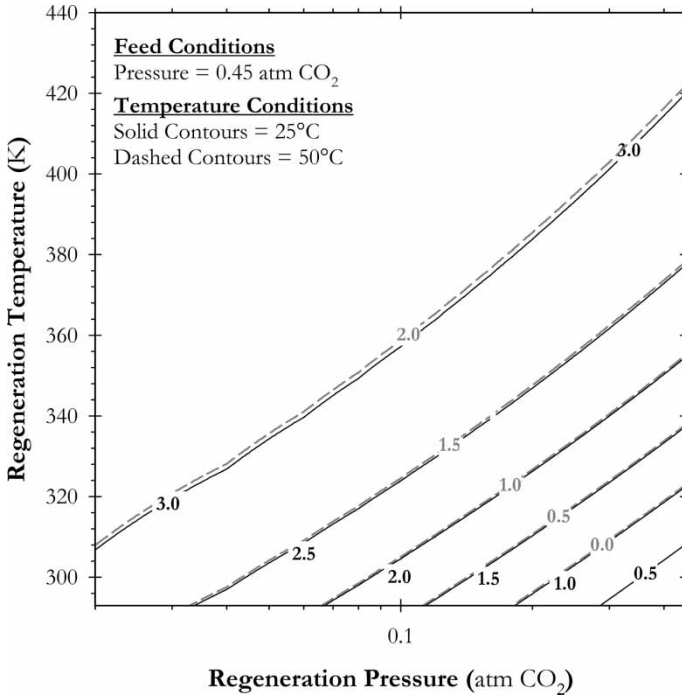

Figure 16. PTSA expected working capacity (mol/kg) for regeneration condition variation with a feed pressure of 0.45 atm CO_2.

difference decreased to 0.7–0.8 mol/kg for the same regeneration temperature and pressure. Therefore, as the feed pressure increases the difference between operating the bed at 25°C or 50°C becomes more pronounced; however, relatively the differences are not large.

CONCLUSIONS

In this study, various CO_2 adsorption isotherms were determined with NaY as the adsorbent. The isotherms were determined in the temperature range of 20°C to 200°C and pressure range of 0.005 to 2.0 atm CO_2 partial pressure. These isotherm data were then fit with a temperature-dependent form of the Toth isotherm. From this data, the Henry's Law constants were determined as a function of temperature and compared to experimental data obtained with the concentration pulse method.

The results show that the temperature-dependent form of the Toth isotherm could fit the experimental isotherm data well. By using this isotherm model, ideal expected working capacities for PSA, TSA, and PTSA cycles were

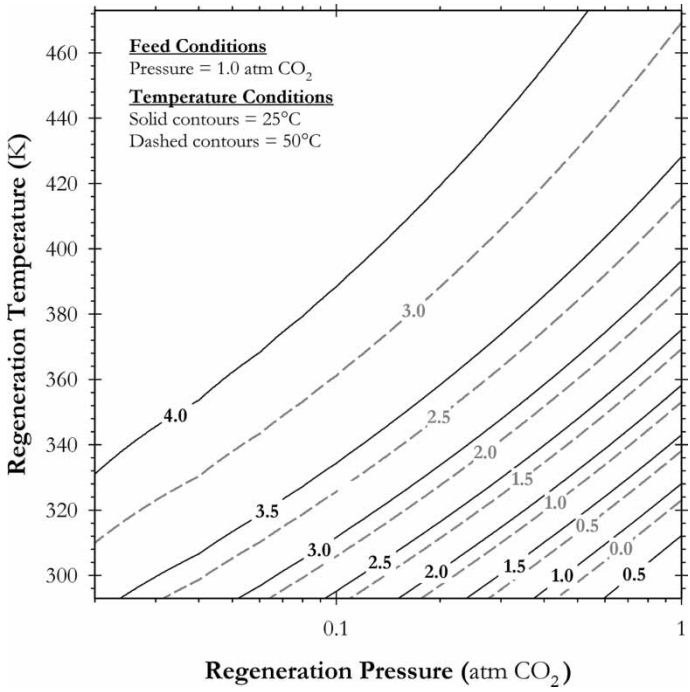

Figure 17. PTSA expected working capacity (mol/kg) for regeneration condition variation with a feed pressure of 1.0 atm CO_2.

studied. The results indicate that the most benefit can be realized by designing a cycle that would exploit the shape factor associated with the adsorption isotherms. For PSA cycles, a higher expected working capacity can be realized, at high regeneration pressures, as the feed temperature increases. This behavior is a result of the shape of the isotherms at the various temperatures.

When used in a TSA cycle at very low bed pressures, the regeneration temperature becomes an independent factor. However, under certain operating conditions, the expected working capacity will increase as the feed temperature increases.

The PTSA cycles showed that the most benefit would be realized with a high pressure and thermal regeneration shock.

NOMENCLATURE

b	Affinity Parameter (1/atm)
b_0	Affinity Parameter at the Reference Temperature (1/atm)
$-\Delta H$	Heat of Adsorption (kJ/mol)

K_p	Henry's Law Constant (mmol/g/atm)
P	Pressure (atm)
Q	Isosteric Heat of Adsorption at the Limit of Zero Coverage (kJ/mol)
q	Amount Adsorbed (mmol/g)
q_m	Limiting Amount Adsorbed (mmol/g)
q_{m0}	Limiting Amount Adsorbed at the Reference Temperature (mmol/g)
R	Gas Constant (kJ/mol/K)
t	Toth Isotherm Parameter (–)
t_0	Toth Isotherm Parameter at the Reference Temperature (–)
T	Temperature (K or °C)
T_0	Reference Temperature (K or °C)

Greek Characters

α	Toth Isotherm Parameter (–)
θ	Coverage (q/q_m^{∞}) (–)
χ	Toth Isotherm Parameter (–)

Abbreviations

CPM	Concentration Pulse Method
GC	Gas Chromatograph
MFC	Mass Flow Controller
SSR	Sum of Square Residuals
TCD	Thermal Conductivity Dectector

ACKNOWLEDGMENTS

Financial support received from the Environmental Science and Technology Alliance Canada (ESTAC) and Natural Sciences and Engineering Research Council (*NSERC*) of Canada are gratefully acknowledged.

REFERENCES

1. Pruschek, R. and Oeljeklaus, G. (1990) Potential CO_2-emission reduction processes. Advances in Solid Fuels Technologies American Society of Mechanical Engineers. *Fuels and Combustion Technologies Division*, 9.
2. Cen, P. and Yang, R.T. (1986) Bulk gas separation by pressure swing adsorption. *Industrial & Engineering Chemistry Fundamentals*, 25 (4).
3. Yang, R.T. (1987) *Gas Separation by Adsorption Processes*; Butterworth Publishers: Mass., U.S.A.
4. Kumar, R. and Van Sloun, J.K. (1989) Purification by adsorptive separation. *Chemical Engineering Progress*, 85 (1).

5. White, D.H., Jr. and Barkley, P.G. (1989) Design of pressure swing adsorption systems. *Chemical Engineering Progress*, 85 (1).
6. Ruthven, D.M., Farooq, S., and Knaebel, K. (1994) *Pressure Swing Adsorption*. VCH Publishers: New York.
7. Inui, T., Okugawa, Y., and Yasuda, M. (1988) Relationship between properties of various zeolites and their CO_2-adsorption behaviors in pressure swing adsorption operation. *Industrial & Engineering Chemistry Research*, 27 (7).
8. Shin, H.S. and Knaebel, K.S. (1988) Pressure swing adsorption: An experimental study of diffusion-induced separation. *AICHE Journal*, 34 (9).
9. Shin, H. (1995) Separation of a binary gas mixture by pressure swing adsorption: Comparison of different PSA cycles. *Adsorption*, 1 (4): 321–333.
10. Sircar, S. and Kratz, W.C. (1988) Simultaneous production of hydrogen and carbon dioxide from steam reformer off-gas by pressure swing adsorption. *Separation Science & Technology*, 23: 14–15.
11. Sircar, S. (1988) Separation of methane and carbon dioxide gas mixtures by pressure swing adsorption. *Separation Science & Technology*, 23: 6–7.
12. Kikkinides, E.S., Yang, R.T., and Cho, S.H. (1993) Concentration and recovery of CO_2 from flue gas by pressure swing adsorption. *Industrial & Engineering Chemistry Research*, 32 (11).
13. Kim, J.N., Chue, K.T., Kim, K.I., Cho, S.H., and Kim, J.D. (1994) Non-isothermal adsorption of nitrogen-carbon dioxide mixture in a fixed bed of zeolite-X. *Journal of Chemical Engineering of Japan*, 27 (1).
14. Chue, K.T., Kim, J.N., Yoo, Y.J., and Cho, S.H. (1995) Comparison of activated carbon and zeolite 13X for CO_2 recovery from flue gas by pressure swing adsorption. *Industrial Engineering Chemistry Research*, 34 (2): 591–598.
15. Dong, F., Lou, H., Kodama, A., Goto, M., and Hirose, T. (1999a) New concept in the design of pressure-swing adsorption processes for multicomponent gas mixtures. *Industrial & Engineering Chemistry Research*, 38 (1).
16. Dong, F., Lou, H., Goto, M., and Hirose, T. (1999b) New PSA process as an extension of the petlyuk distillation concept. *Separation & Purification Technology*, 15 (1).
17. Warmuzinski, K. and Sodzawiczny, W. (1999) Effect of adsorption pressure on methane purity during PSA separations of CH_4/N_2 mixtures. *Chemical Engineering & Processing*, 38 (1).
18. Suh, S.-S. and Wankat, P.C. (1989) New pressure swing adsorption process for high enrichment and recovery. *Chemical Engineering Science*, 44 (3).
19. Gladden, L.F. (1991) Influence of pellet structure on selectivity during pressure swing adsorption separations. *Chemical Engineering Science*, 46 (10).
20. Alpay, E., Kenney, C.N., and Scott, D.M. (1994) Adsorbent particle size effects in the separation of air by rapid pressure swing adsorption. *Chemical Engineering Science*, 49 (18).
21. Buzanowski, M.A., Yang, R.T., and Haas, O.W. (1989) Direct observation of the effects of bed pressure drop on adsorption and desorption dynamics. *Chemical Engineering Science*, 44 (10).
22. Farooq, S., Hassan, M.M., and Ruthven, D.M. (1988) Heat effects in pressure swing adsorption systems. *Chemical Engineering Science*, 43 (5).
23. Kumar, R. (1995) Effect of variable feed concentration on the performance of a pressure swing adsorption process. *Adsorption*, 1 (3): 203–211.
24. Matz, M.J. and Knaebel, K.S. (1988) Pressure swing adsorption: Effects of incomplete purge. *AICHE Journal*, 34 (9).

25. Harlick, P.J.E. and Tezel, F.H. (2004) An adsorbent screening study for CO_2 removal from N_2. *Microporous and Mesoporous Materials*, 79: 71–79.
26. Do, D.D. (1998) *Adsorption Analysis: Equilibria and Kinetics*; Series in Chemical Engineering, Imperial College Press: UK; Vol. 2.
27. Habgood, H.W. (1964) Adsorptive and gas chromatographic properties of various cationic forms of zeolite X. *Canadian Journal of Chemistry*, 42: 2340–2350.
28. Van der Vlist, E. and Van der Meijden, J. (1973) Determination of the adsorption isotherms of the components of binary gas mixtures by gas chromatography. *Journal of Chromatography*, 79: 1–13.
29. Shah, D.B. and Ruthven, D.M. (1977) Measurement of zeolitic diffusivities by chromatography. *AIChE Journal*, 23 (6).
30. Hyun, S.H. and Danner, R.P. (1982) Determination of gas adsorption equilibria by the concentration-pulse technique. *AIChE Symp. Ser.*, 34 (11).
31. Buffman, B.A., Mason, M., and Yadav, G.D. (1985) Retention volumes and retention times in binary chromatography. *J. Chem. Soc., Faraday Trans. I*, 81: 161–173.
32. Buffman, B.A., Mason, G., and Heslop, M.J. (1999) Binary adsorption isotherms from chromatographic retention times. *Ind. Eng. Chem. Res.*, 38 (3): 1114–1124.
33. Kabir, H., Grevillot, G., and Tondeur, D. (1998) Equilibria and activity coefficients for non-ideal adsorbed mixtures from perturbation chromatography. *Chemical Engineering Science*, 53 (9): 1639–1654.
34. Mason, G. and Buffman, B.A. (1996) Gas adsorption isotherms from composition and flow-rate transient times in chromatographic columns II. Effect of pressure changes. *Proc. R. Soc. Lond. A*, (452): 1287–1300.
35. Hyun, S.H. and Danner, R.P. (1985) *Gas* adsorption isotherms by use of perturbation chromatography. *Industrial Engineering Chemistry Fundamentals*, 24: 95–101.
36. Harlick, P.J.E. and Tezel, F.H. (2000) A novel solution method for interpreting binary adsorption isotherms from concentration pulse chromatography data. *Adsorption*, 6 (4): 293–309.
37. Harlick, P.J.E. and Tezel, F.H. (2001) The importance of experimental data regression for interpreting binary adsorption isotherms from concentration pulse chromatography data: A novel functional set. *Canadian Journal of Chemical Engineering*, 79: 236–245.
38. Harlick, P.J.E. and Tezel, F.H. (2002) Adsorption of carbon dioxide, methane and nitrogen: Pure and binary mixture adsorption by ZSM-5 with low SiO_2/Al_2O_3 ratio. *Separation Science and Technology*, 37 (1): 33–60.